Desalination and Water Treatment
www.deswater.com

doi: 10.5004/dwt.2017.21466

92 (2017) 134–144
October

Facile synthesis of aluminum-based bimetallic (hydr)oxides for enhanced fluoride removal from water

Qiongzhi Tang[a,b], Haiying Wang[a,c], Shunqi Tian[a], Ruiyang Xiao[a,c], Liyuan Chai[a,c], Weichun Yang[a,c,*]

[a]*Department of Environmental Engineering, School of Metallurgy and Environment, Central South University, Changsha, Hunan 410083, China, Tel. +86 731 88830875; Fax: +86 731 88710171; email: yang220@csu.edu.cn (W. Yang)*
[b]*Yongzhou Environment Protection Agency, Yongzhou, Hunan 425000, China*
[c]*Chinese National Engineering Research Center for Control and Treatment of Heavy Metal Pollution, Changsha, Hunan 410083, China*

Received 29 March 2017; Accepted 19 September 2017

ABSTRACT

Various aluminum-based bimetallic (hydr)oxides including Mn, Zn, Cu, Ce, Bi, Zr and La have been synthesized in single-step coprecipitation without high energy consumption. The characterization of Ce–Al (hydr)oxides and La–Al (hydr)oxides was undertaken by scanning electron microscopy with an energy dispersive X-ray spectroscopy, zeta potential measurement, X-ray powder diffractometer and N_2 adsorption/desorption analysis. The tendency of fluoride affinity to these aluminum-based bimetallic (hydr)oxides confirmed that the fluoride removal of the various composites decreased with the augment of the electronegativity of the anchored metals. Ce–Al (hydr)oxides and La–Al (hydr)oxides have better potential of fluoride removal from aqueous solution with adsorption capacity of 105.05 and 86.48 mg g^{-1} calculated from Langmuir model. The high fluoride removal performance was attributed to the fact that both Ce and La atoms can act as a bridge between adsorbed fluoride and adsorbents surface while the main role for Al atoms was to form an amorphous structure. The regeneration confirmed that Ce–Al (hydr)oxides have good reusability in fluoride removal after the five recycle. The results indicate that the Ce–Al (hydr)oxides composites could be preferably used as an effective adsorbent for fluoride removal from aqueous solution.

Keywords: Aluminum-based bimetallic (hydr)oxides; Ce–Al (hydr)oxides; La–Al (hydr)oxides; Fluoride removal

1. Introduction

Fluoride contamination in water has been recognized as a worldwide problem, and its concentration in drinking water at many places of the world exceeds the permissible limits [1–3]. People living in places where water has high concentrations of fluoride are affected by fluorosis, which is one of the most frequently occurring endemic diseases [4–7]. In China, the spread area with drinking-water endemic fluorosis covers about 2.2 million km^2 [8]. India and Mexico also suffer from same serious problems due to high fluoride concentration in drinking water [9].

Conventional methods for fluoride removal generally include precipitation, electrocoagulation and adsorption [2,7,10]. Adsorption has been considered as one of the most effective, economic and environment-friendly for the removal of low-concentration aqueous contaminants [11–14]. Among the oxides and hydroxides of metal ions that have been widely used for fluoride removal, the oxides and hydroxides of aluminum are the most promising candidate due to the high binding affinity, selectivity for fluoride and cost-effectiveness [15,16]. However, poor fluoride adsorption capacity narrowed their applications significantly, mostly followed by secondary pollution from dissolution of aluminum [17,18].

Practically, multimetallic Al-based composites may be increasingly important alternative by not only inheriting the

* Corresponding author.

advantages of parent (hydr)oxides but also showing obviously synergistic effects. To date, many recent researches were implicated in formation of multimetallic (hydr)oxides [19], such as CaO/Al_2O_3 [20], CeO_2/Al_2O_3 [21], Mg–Al bimetallic oxides [22], Mg–Al layered double hydroxides [23], MnO_2/Al_2O_3 [24], Al_2O_3–ZrO_2 [25], Fe–Al–Ce trimetal hydrous oxide [26], Ca–Al–La composite [27] and Al–Fe (hydr)oxides [28]. These composites all exhibited enhanced fluoride removal performance. For instance, CaO loaded mesoporous Al_2O_3 by Dayananda et al. [20] showed higher fluoride adsorption capacity and faster kinetics than mesoporous Al_2O_3. Jia et al. [29] synthesized a novel composite of two-line ferrihydrite/bayerite with fluoride adsorption capacity of 123.03 mg g^{-1} at pH 7.0 higher than that of individual iron (or aluminum) hydroxide.

Based on the above discussion, it can be concluded that the fluoride adsorption capacity of aluminum (hydr)oxide could be increased by chemical modification of its surfaces. As the fluoride ion is classified as a hard base, it has a strong affinity toward multivalent metal ions such as Ce^{4+}, La^{3+}, Zr^{4+}, Zn^{2+}, etc. [30–32]. Impregnation of multivalent metal ions (such as Ce^{4+}, La^{3+}, Zr^{4+} and Zn^{2+}) onto the aluminum-based adsorbent can help to create positive charges on the adsorbent surface and improve the affinity for fluoride, resulting in the improvement of fluoride adsorption capacity [20,33]. However, development of aluminum contained metal (hydr) oxides composites with high fluoride adsorption capacity still relies on experience because of lack of thorough understanding of fluoride adsorption mechanism. Elucidation of the effect of multivalent metal ions on the fluoride adsorption behavior will greatly promote the understanding of adsorption mechanisms. Moreover, the synthesis procedure for the aluminum-based mixed composites is complicated, and typically accomplished in two (or three) steps or high temperature calcination. For example, the Mg–Al bimetallic oxides as reported by Moriyama et al. [22] were synthesized from hydrotalcite using increasing calcination temperatures (873, 1,073, 1,273 K); in the preparation of CaO loaded mesoporous Al_2O_3 by Dayananda et al. [20], the first step involves the synthesis of mesoporous Al_2O_3, and the next step involves a wet impregnation technique. The synthesis procedures for the aluminum-based mixed composites should be simplified.

The primary objectives of the present study were to (i) compare the fluoride adsorption performance of a series of aluminum-based bimetallic (hydr)oxides synthesized in single-step without high energy consumption; (ii) obtain aluminum-based composites adsorbents with high fluoride adsorption capacity, wide available pH range in water treatment; and (iii) illustrate the predominant nature of the interactions between aluminum-based bimetallic (hydr)oxides and fluoride.

2. Materials and methods

2.1. Sample preparation

The composites were synthesized by a coprecipitation method using aluminum sulfate and other metal salts such as cerium nitrate, lanthanum chloride, zinc nitrate and copper chloride. In a typical synthesis procedure, 0.1 M of $Al_2(SO_4)_3{\cdot}18H_2O$ and 0.02 M metal salts (such as $Ce(NO_3)_3{\cdot}6H_2O$) were dissolved in deionized water. The added mole ratio of Al:metal (e.g., Mn, Zn, Cu, Ce, Bi, Zr and La) is 10:1. Solution pH was adjusted to 11.0 by dropwise addition of 2.0 M NaOH solution under vigorous stirring at room temperature of 25°C. Then, the mixture was stirred over a period of 6 h. During the process, the pH of the mixture was maintained at 11.0 using 0.1 M NaOH solutions. Afterwards, the resulting mixture was filtered, washed with deionized water for several times, and dried at 80°C for 24 h to obtain the composites adsorbents.

2.2. Characterization of adsorbents

The surface morphologies and chemical compositions were studied by JEOL JSM-6335F scanning electron microscopy (SEM) with an energy dispersive X-ray spectroscopy (EDX) detector. X-ray diffraction analysis was performed on Rigaku-TTR III powder diffractometer to obtain the composition crystalline structures of adsorbents. Zeta potentials of the adsorbents were determined by a zeta potential meter (Malvern Zetasizer Nano ZS90, Malvern Instrument Co., Ltd., UK). Fourier transform infrared spectroscopy (FTIR) spectra of the product was obtained using a Nicolet IS10 spectrometer (Thermo Fisher, USA) in the wavenumber range of 400–4,000 cm^{-1} with 4 cm^{-1} resolution. The textural properties of the materials were determined by Brunauer–Emmett–Teller (BET) N_2 adsorption–desorption analysis using a micrometrics surface area analyzer (Autosorbi/monosorb, Quantachrome, USA). The surface of adsorbents before and after fluoride adsorption was analyzed using X-ray photoelectron spectroscopy (XPS, K-Alpha 1063 Ultra spectrometer, Thermo Fisher Scientific, UK) with a monochromatic Al Kα X-ray source (1,486.71 eV).

2.3. Adsorption experiments

All the adsorption experiments were performed in 120 mL polyethylene vials filled with 100 mL aqueous fluoride solution, and an adsorbent dose of 1 g L^{-1} was added. The vials were placed in thermostatic water bath and shaken for 24 h at 25°C, afterwards, the samples were filtered and the fluoride concentrations in solutions were analyzed with a fluoride-selective electrode by using total ionic strength adjustment buffer solution to eliminate the interference of complexing ions.

Batch experiments for fluoride removal by various aluminum-based bimetallic (hydr)oxides were conducted with initial fluoride concentration of 40 mg L^{-1} at solution pH 4.5 ± 0.2. For the selected aluminum-based bimetallic (hydr) oxides. For kinetics experiment, adsorption reaction time was selected from 5 to 1,440 min with two initial fluoride concentrations (9.11 and 38.32 mg L^{-1}). In the isotherm experiment, the initial fluoride concentration varies from 2 to 170 mg L^{-1} at pH 4.5 ± 0.1. The effects of pH on fluoride adsorption were examined by adjusting initial solution pH from 2 to 12 using 0.1 M HCl and 0.1 M NaOH with initial fluoride concentrations of 30 mg L^{-1}, the aqueous concentrations of fluoride were determined after adsorption. To explore the regeneration and reuse, the adsorbent was added into the 40 mg L^{-1} fluoride solution following the adsorption experiment. Afterwards the adsorbent was filtered and dispersed in 100 mL 0.005 M

NaOH solution under stirring for 2 h for regeneration. The obtained adsorbent was used for the next adsorption or reuse cycle. Each experiment was carried out in duplicate to obtain reproducible results with an error less than 5%.

3. Results and discussion

3.1. Fluoride removal potential of aluminum-based bimetallic (hydr)oxides

Possibility of fluoride removal by various aluminum-based bimetallic (hydr)oxides has been examined. Fig. 1 shows the results of fluoride removal from aqueous solutions by various aluminum-based bimetallic (hydr)oxides with initial fluoride concentration of 40 mg L^{-1} at pH 4.5. Obviously, the incorporation of multivalent metal can significantly impact the fluoride adsorption on aluminum-based (hydr)oxides, the adsorbed amount for the various aluminum-based bimetallic (hydr)oxides were in the following order: Ce–Al (hydr) oxides > La–Al (hydr)oxides > Zr–Al (hydr)oxides > Zn–Al (hydr)oxides > Cu–Al (hydr)oxides > Mn–Al (hydr)oxides > Bi–Al (hydr)oxides. The Ce–Al (hydr)oxides and La–Al (hydr) oxides have better potential of fluoride removal from aqueous solution with adsorbed amount of 34.41 and 24.50 mg g^{-1}, respectively, while the adsorbed amount for Bi–Al (hydr) oxides is only 3.56 mg g^{-1}. As the mole ratio of the incorporated multivalent metal:Al is 1:10 in the synthesis process, it is suggested that the fluoride adsorption on Ce–Al (hydr)oxides and La–Al (hydr)oxides was mainly due to the incorporated Ce and La. A closely related property is electronegativity of the metal elements. Fluorine is the most electronegative element with the value of 3.98 and it can stably bonded to the atom with the low electronegativity [34]. In general, the adsorbed amount for the various aluminum-based bimetallic (hydr)oxides decreased with the increase of the electronegativity of the metals contained in the aluminum-based bimetallic (hydr)oxides (Table 1). Ce and La have the lower electronegativity among these metals, and exhibit a stronger attraction toward fluorine atom. This can be used to explain why Ce–Al (hydr)oxides and La–Al (hydr)oxides showed better performance for fluoride removal. Characterization and adsorption experiments of Ce–Al (hydr)oxides and La–Al (hydr)oxides were undertaken to understand the possible adsorption mechanisms and useful properties of the material toward intended objective.

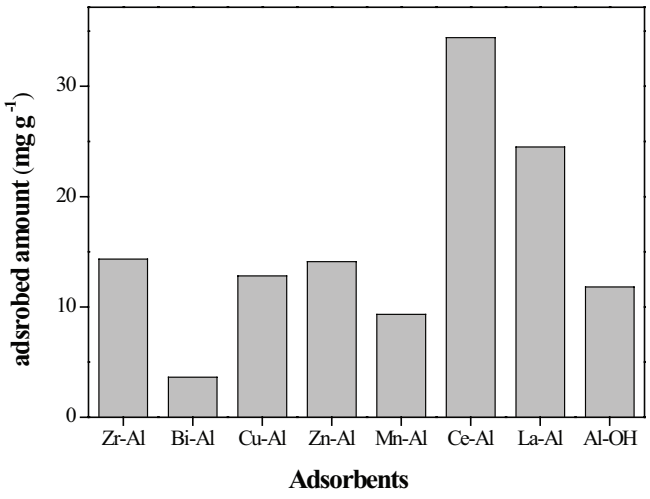

Fig. 1. Fluoride removal from water by different aluminum-based mixed (hydr)oxides, Zr–Al, Bi–Al, Cu–Al, Zn–Al, Mn–Al, Ce–Al, La–Al and Al–OH represent Zr–Al (hydr)oxides, Bi–Al (hydr) oxides, Cu–Al (hydr)oxides, Zn–Al (hydr)oxides, Mn–Al (hydr) oxides, Ce–Al (hydr)oxides, La–Al (hydr)oxides and $Al(OH)_3$, respectively.

3.2. Characteristic of adsorbents

SEM micrographs of Ce–Al (hydr)oxides and La–Al (hydr)oxides are shown in Fig. 2. The forms and shapes of Ce–Al (hydr)oxides particles (Fig. 2(a)) exhibited agglomerated particle structures, while the SEM image of La–Al (hydr) oxide (Fig. 2(c)) shows crumpled morphology with stacked layers. EDX spectra (Figs. 2(b) and (d)) confirm the presence of Ce and La elements in Ce–Al (hydr)oxides and La–Al (hydr)oxides, respectively. X-ray powder diffractometer (XRD) patterns of the materials (Fig. 3) illustrate that characteristic peaks of $Al(OH)_3$ (bayerite, JCPDS cards no. 20-0011) were identified in both Ce–Al (hydr)oxides and La–Al (hydr) oxides. Further, the peaks at 28.55°, 33.08°, 47.49° and 56.35° could be assigned to CeO_2 (JCPDS cards no. 75-0120) [35] for Ce–Al (hydr)oxides (Fig. 3(a)), and the peaks at 26.2°, 27.8°, 30.0° and 46.2° could be assigned to La_2O_3 (JCPDS File No. 65-3185) for La–Al (hydr)oxides [36]. The pH_{PZC} of Ce–Al (hydr)oxides and La–Al (hydr)oxides determined by zeta potential were 10.93 and 8.9, respectively. The BET specific surface areas and total pore volumes were 23.78 m^2 g^{-1} and 0.079 cm^3 g^{-1} for Ce–Al (hydr)oxides, and 35.88 m^2 g^{-1} and 0.159 cm^3 g^{-1} for La–Al (hydr)oxides, respectively. The N_2 adsorption–desorption isotherm and pore-size distribution curve (Fig. 4) implied the existence of micropores in both Ce–Al (hydr)oxides and La–Al (hydr)oxides.

3.3. Adsorption kinetics

The adsorption kinetic data of fluoride on Ce–Al (hydr) oxides and La–Al (hydr)oxides at pH 4.5 and the fit model curves are shown in Figs. 5 and 6. It can be found that most of the adsorption took place in the first 60 min, and then the adsorption increased gradually until the equilibrium was reached. The pseudo-first-order kinetic equation (Eq. (1)) and pseudo-second-order kinetic equation (Eq. (2)) were applied to fit the adsorption the kinetic data.

Table 1
The electronegativity of the metal and fluorine elements

Element	Electronegativity
Mn	1.55
Cu	1.90
Zn	1.65
Zr	1.33
La	1.11
Ce	1.12
Bi	2.02
F	3.98

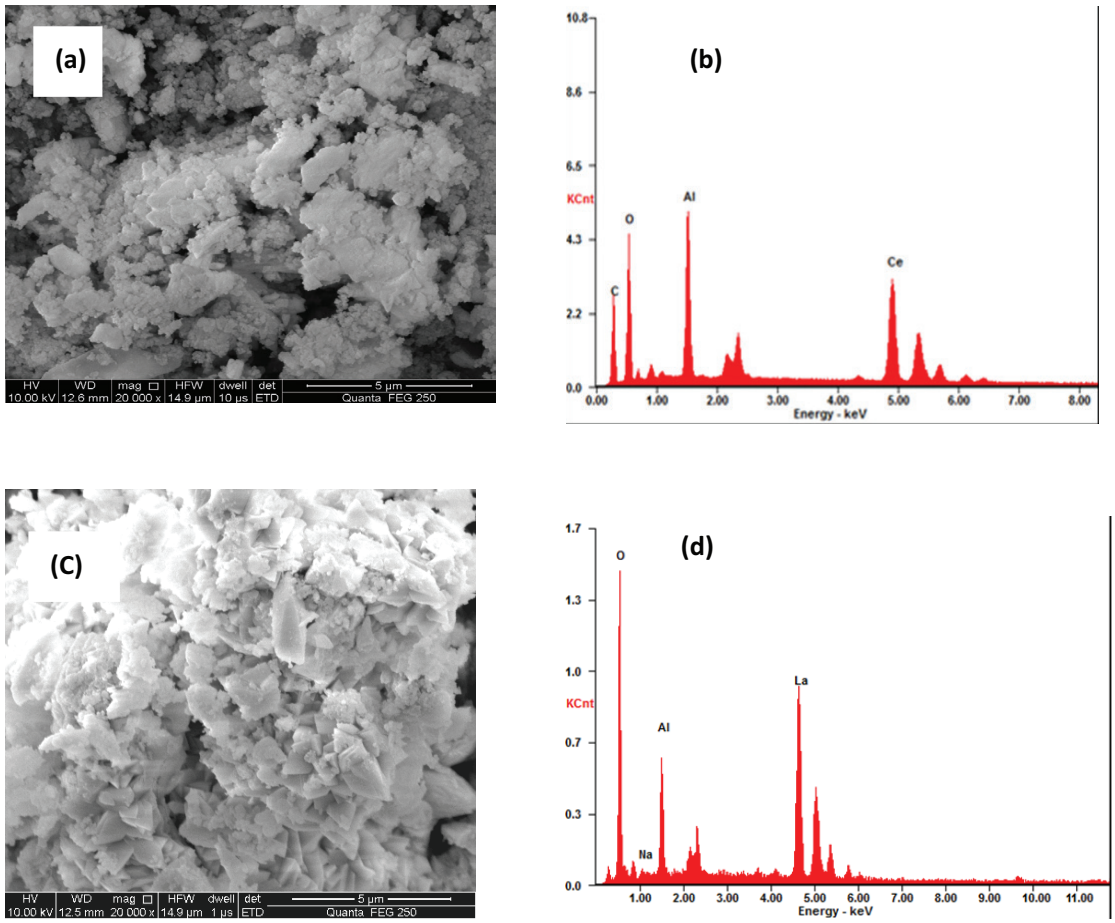

Fig. 2. SEM images with EDS spectra of (a) and (b) Ce–Al (hydr)oxides and (c) and (d) La–Al (hydr)oxides.

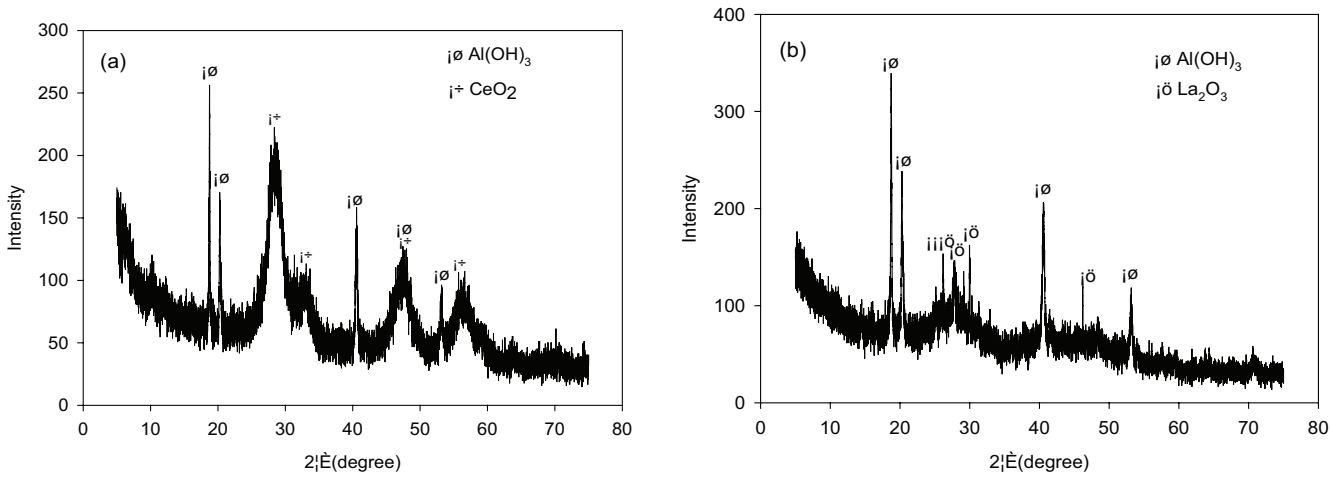

Fig. 3. XRD patterns of (a) Ce–Al (hydr)oxides and (b) La–Al (hydr)oxides.

$$\log(q_e - q_t) = \log q_e - \frac{k_1 t}{2.303} \quad (1)$$

$$\frac{t}{q_t} = \frac{1}{k_2 q_e^2} + \frac{t}{q_e} \quad (2)$$

where t is the reaction time (min), q_e (mg g^{-1}) and q_t (mg g^{-1}) are the amount of adsorbed fluoride at equilibrium and at any reaction time t, k_1 (min^{-1}) and k_2 (g mg^{-1} min^{-1}) are the equilibrium rate constants for pseudo-first-order and pseudo-second-order models, respectively.

The fits of the two models to the fluoride adsorption kinetic data for Ce–Al (hydr)oxides and La–Al (hydr)oxides

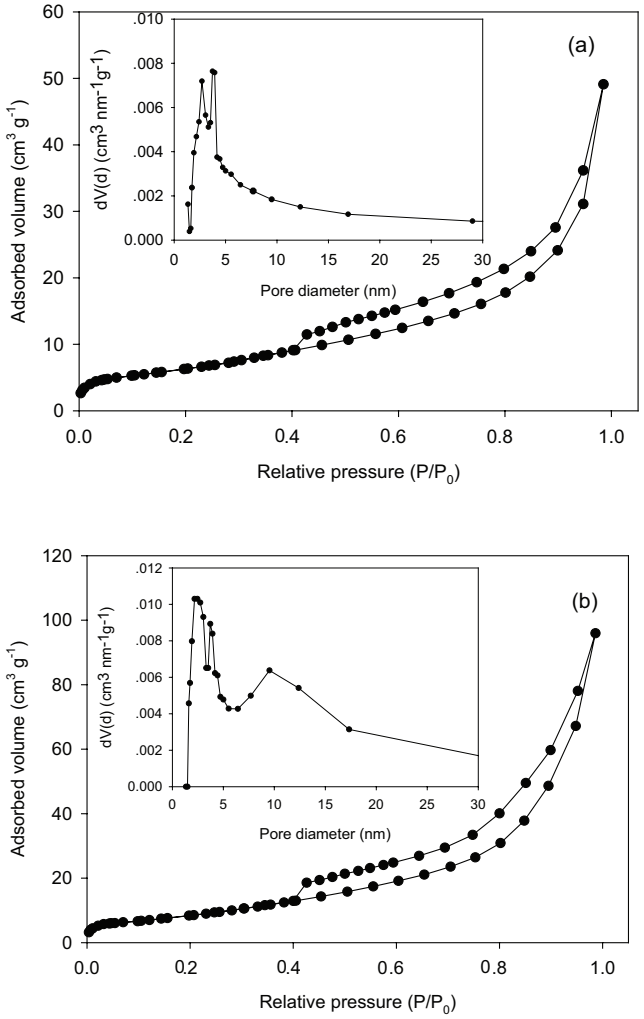

Fig. 4. N_2 adsorption desorption isotherms and Barrett–Joyner–Halenda pore-size distribution (inset) of (a) the Ce–Al (hydr) oxides and (b) La–Al (hydr)oxides.

are shown in Figs. 5 and 6, respectively. The model parameters obtained by curve-fitting kinetic data are listed in Table 2. The pseudo-second-order fitted better for the fluoride adsorption kinetics than pseudo-second-order model. It means that the "surface reaction" was dominated and controlled adsorption stage. The rate-limiting step may be due to the chemisorptions involving the desorption of –OH from the adsorbent surface and the effective collision of fluoride ions. The rate constant k_2 for Ce–Al (hydr)oxides was much higher than that for La–Al (hydr)oxides, indicating the much faster adsorption kinetics of fluoride on Ce–Al (hydr)oxides than on La–Al (hydr)oxides.

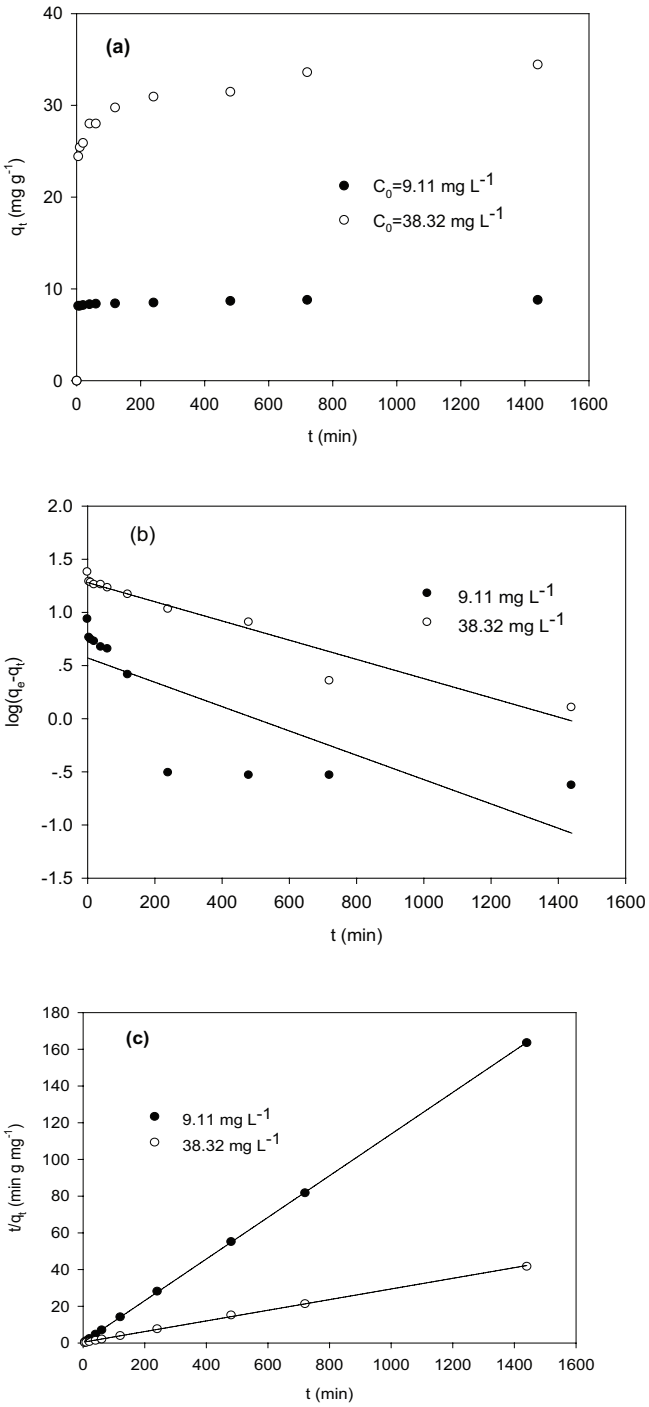

Fig. 5. (a) Effect of reaction time on fluoride adsorption on Ce–Al (hydr)oxides, kinetics modeling of fluoride adsorption; (b) pseudo-first-order kinetic plots; (c) pseudo-second-order kinetic plots.

3.4. Effect of solution pH on fluoride removal

The effect of solution pH on fluoride removal by Ce–Al (hydr)oxides and La–Al (hydr)oxides was studied in the pH range of 3.0–12.0 (Fig. 7). The Ce–Al (hydr)oxides exhibited a considerably high adsorption capacity over a relatively wide pH range, for example, the fluoride removal efficiencies reached up to 90% throughout the pH range of 4–11. The relatively wide optimum adsorption pH was possibly related to the high pH_{PZC} of Ce–Al (hydr)oxide (10.93). However, maximum fluoride removal (98.3%) was achieved at pH 3 and the minimum (8.7%) was at pH 12 for La–Al (hydr)oxides. The reduction in the concentration of fluoride in the alkaline pH range could be attributed to competition of hydroxyl ions with fluoride for the

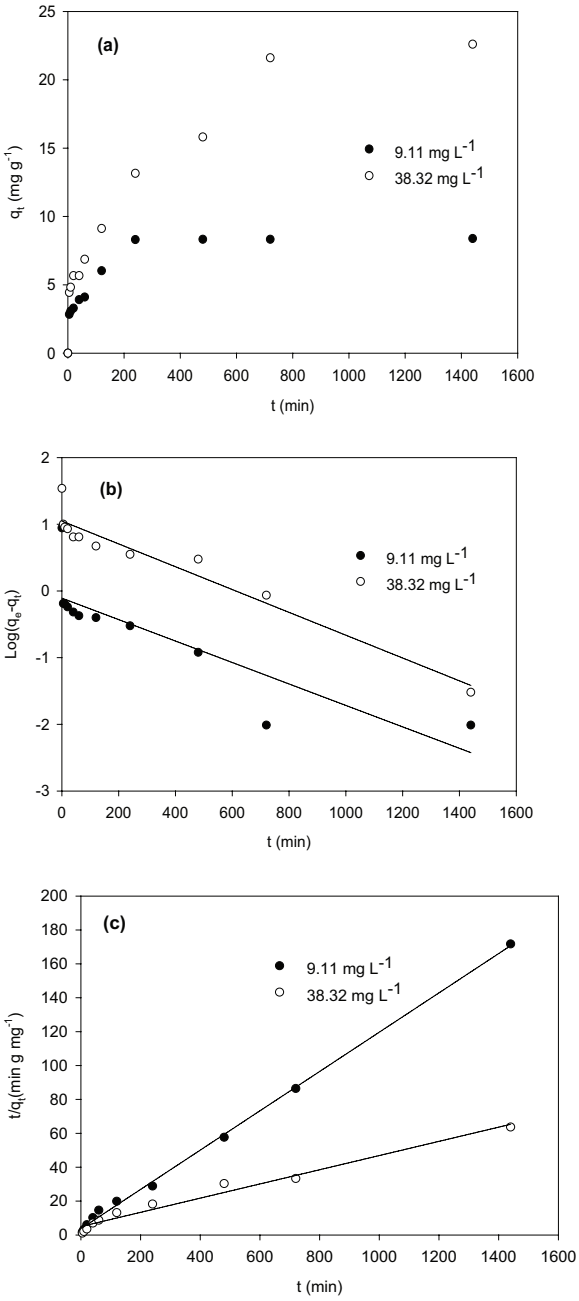

Fig. 6. (a) Effect of reaction time on fluoride adsorption on La–Al (hydr)oxides, kinetics modeling of fluoride adsorption; (b) pseudo-first-order kinetic plots; (c) pseudo-second-order kinetic plots.

adsorption sites. It is clearly indicated that Ce–Al (hydr)oxides performs better in fluoride removal at various pH than La–Al (hydr)oxides. And the wider optimum pH range is favorable to the application of Ce–Al (hydr)oxides for fluoride removal in aqueous environment.

3.5. Adsorption isotherm

The fluoride adsorption isotherm for Ce–Al (hydr)oxides and La–Al (hydr)oxides at pH 4.5 is shown in Fig. 8. The aluminum concentrations released in the solution were about

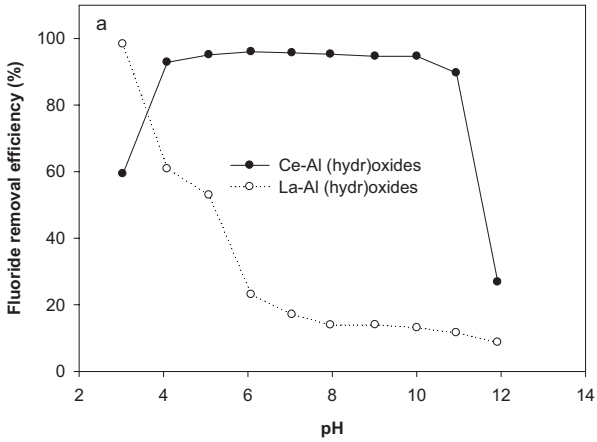

Fig. 7. Effect of pH on fluoride removal by Ce–Al (hydr)oxides and La–Al (hydr)oxides with fluoride concentration at 30 mg L^{-1}.

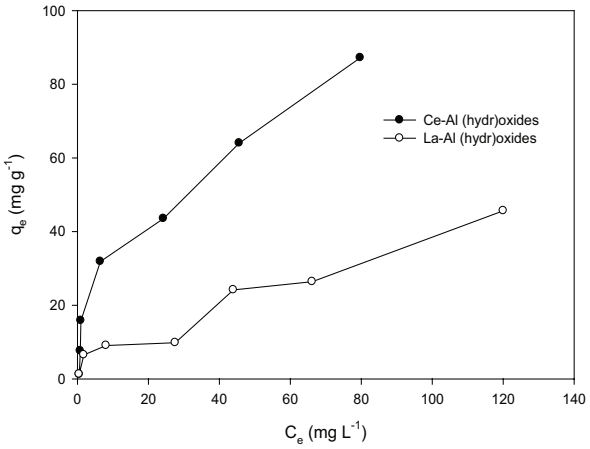

Fig. 8. Adsorption isotherms of fluoride on Ce–Al (hydr)oxides and La–Al (hydr)oxides.

Table 2
Kinetic and statistical parameters of two kinetic models

Adsorbents	Data set (mg L^{-1})	Pseudo-first-order model			Pseudo-second-order model		
		q_e	k_1	R^2	q_e	k_2	R^2
Ce–Al (hydr)oxides	9.11	0.78	3.68×10^{-3}	0.731	8.81	3.52×10^{-2}	1.000
	38.32	11.17	3.92×10^{-3}	0.933	34.48	2.00×10^{-3}	0.999
La–Al (hydr)oxides	9.11	3.73	2.53×10^{-3}	0.633	8.62	3.65×10^{-3}	0.998
	38.32	19.10	2.07×10^{-3}	0.939	23.87	3.51×10^{-4}	0.975

0.1–0.2 mg L^{-1} at pH 4.5, which are lower than the value of 0.2 mg L^{-1} proposed by World Health Organization (WHO). The Langmuir (Eq. (3)), Redlich–Peterson (Eq. (4)) and Sips (Eq. (5)) models were used to fit the adsorption isotherms.

$$q_e = \frac{q_m b C_e}{1 + b C_e} \tag{3}$$

$$q_e = \frac{K_R C_e}{1 + \alpha_R C_e^{\beta}} \tag{4}$$

$$q_e = \frac{q_m (K_S C_e)^m}{1 + (K_S C_e)^m} \tag{5}$$

where q_e (mg g^{-1}) is the amount of fluoride adsorbed per mass of adsorbent; C_e (mg L^{-1}) is the concentration of fluoride at equilibrium; b is the equilibrium adsorption constant related to the affinity of binding sites (L mg^{-1}); q_m is the maximum amount of the fluoride per unit mass of adsorbent, K_R (L mg^{-1}), β and α_R (L mg^{-1}) are Redlich–Peterson constants; K_S (L mg^{-1}) in Sips model is the affinity constant for fluoride adsorption.

The adsorption parameters obtained from the isotherms are presented in Table 3. Sips model fitted better to the fluoride adsorption, indicating that fluoride adsorption takes place on both homogenous and heterogeneous surface of the adsorbents. The adsorption capacity calculated from Langmuir model was 105.05 and 86.48 mg g^{-1} for Ce–Al (hydr)oxides and La–Al (hydr)oxides, respectively. The comparison of fluoride adsorption capacities with some other adsorbents (Table 4) had also suggested that the Ce–Al (hydr) oxides and La–Al (hydr)oxides composites developed in the present study are highly competitive for fluoride removal.

3.6. Regeneration

The regeneration and recyclability of Ce–Al (hydr)oxides were evaluated through five regeneration cycles with initial fluoride concentration of 40 mg L^{-1}, and the results are shown in Fig. 9. The fluoride removal efficiency did not change much and was around 70% during five regeneration cycles. The results demonstrate that the as-prepared Ce–Al (hydr) oxides could be well regenerated via NaOH treatment, and can still exhibit good adsorption performance even after five cycles of adsorption–desorption.

3.7. Adsorption mechanism

FTIR spectra of Ce–Al (hydr)oxides and La–Al (hydr) oxides before and after fluoride adsorption are shown in

Table 3
Parameters of the fitting of different isotherm models to the experimental data for fluoride adsorption on Ce–Al (hydr)oxides and La–Al (hydr)oxides

Adsorbents	Langmuir model			Redlich–Peterson model				Slips model			
	q_m (mg g^{-1})	b (L mg^{-1})	R^2	K_R (L mg^{-1})	α_R (L mg^{-1})	β	R^2	q_m (mg g^{-1})	K_S (L mg^{-1})	m	R^2
Ce–Al (hydr)oxides	105.05	0.0415	0.932	89.23	7.70	0.543	0.976	200.43	0.0069	0.607	0.980
La–Al (hydr)oxides	86.48	0.0085	0.950	18.79	13.97	0.263	0.951	145.25	0.0045	0.720	0.961

Table 4
Comparison of fluoride adsorption capacity of various adsorbents

Adsorbent	Amount adsorbed (mg g^{-1})	Experimental conditions	Reference
Mg-Al-LDH	>32.4	pH 5.0	[37]
Ca–Al–La composite	29.30	pH 6.8 ± 0.2	[27]
Bayerite/boehmite	56.8	pH 7.0	[38]
Fungus hyphae-supported alumina	105.60	pH 6.0	[39]
Alum-impregnated activated alumina	40.68	pH 6.5	[40]
Hydrated iron(III)–aluminum(III)–chromium(III) ternary mixed oxide (HIACMO)	31.89	pH 5.6 ± 0.2	[41]
Polypyrrole/Fe_3O_4	17.6–22.3	pH 6.5	[42]
Sulfate-doped Fe_3O_4/Al_2O_3	70.4	pH 7.0	[43]
Metal-organic frameworks	41.36	pH 6–9	[44]
Nanoalumina	14.0	pH 6.15	[45]
α-FeOOH@rGO	24.67	–	[46]
Fe_3O_4@Alg-La particles	45.23	pH 4.0	[47]
Ce–Al (hydr)oxides	105.05	pH 4.5	This study
La–Al (hydr)oxides	86.48	pH 4.5	This study

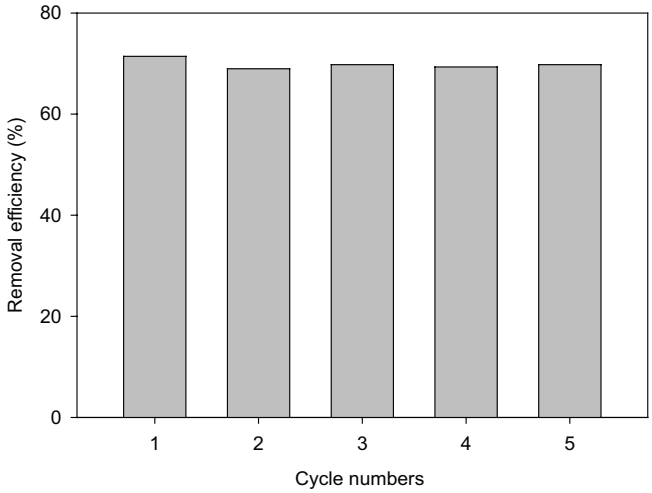

Fig. 9. Recycling behavior of Ce–Al (hydr)oxides, initial fluoride concentration 40 mg L^{-1}; adsorbent dose 1 g L^{-1}; shaking time 10 h; pH = 7.

Fig. 10. For the pristine adsorbents, the peaks between 3,550–3,200 cm^{-1} and near 1,600 cm^{-1} could be attributed to HOH stretching and bending vibration of water, respectively [48]. As shown in Fig. 10(a), a band at 538 cm^{-1} can be assigned to Ce–OH vibrations, and it disappeared after fluoride adsorption, which corroborated the interaction of fluoride with the Ce–OH on the adsorbent. Meanwhile, the disappearance of the peaks at about 667 and 560 cm^{-1} (Fig. 10(b)) associated with La–OH bond vibrations indicates that the La–OH were involved in the fluoride adsorption [27,49]. From this evidence, a ligand exchange relationship between the three metal–OH groups and F ions was found. The loading of Ce and La onto the adsorbents significantly change the adsorbents surface which in favor of fluoride adsorption and improves fluoride adsorption capacity. Both Ce and La atoms can act as a bridge between adsorbed fluoride and adsorbents surface.

Surface structure information of Ce–Al (hydr)oxides and La–Al (hydr)oxides was analyzed by XPS before and after fluoride adsorption. The XPS spectra of Ce 3d, La 3d and Al 2p are shown in Fig. 11. For the Ce 3d spectrum, the peaks at 882.3 and 898.6 eV were considered to belong to Ce(IV) $3d_{5/2}$ and Ce(IV) $3d_{3/2}$, while the peaks at 885.6 and 904.8 eV were due to Ce(III) $3d_{5/2}$ and Ce(III) $3d_{3/2}$. After fluoride adsorption, the binding energy of Ce(IV) $3d_{5/2}$ was shifted from 882.3 to 882.1 eV and Ce(IV) $3d_{3/2}$ was shifted from 898.6 to 898.1 eV for Ce(IV); the binding energy of Ce(III) $3d_{5/2}$ was shifted from 885.6 to 884.1 eV and Ce(III) $3d_{3/2}$ was shifted from 904.8 to 903.7 eV; indicating the occurrence of strong interactions between fluoride and Ce atoms. Fig. 11(b) shows the characteristic spectrum of La 3d exhibits two asymmetric lines at 838.7 eV (La $3d_{5/2}$) and 855.6 eV (La $3d_{3/2}$) with their satellites at 835.3 and 852.0 eV, respectively. After fluoride adsorption, the binding energy of La $3d_{3/2}$ was shifted to 855.0 eV; and the satellites of La $3d_{5/2}$ were shifted from 835.3 to 835.8 eV, indicating that the La is involved in fluoride adsorption. While the peak shapes of Al 2p and the binding energy peak for both Ce–Al (hydr)oxides and La–Al (hydr) oxides (Figs. 11(c) and (d)) did not change much. Thus, the

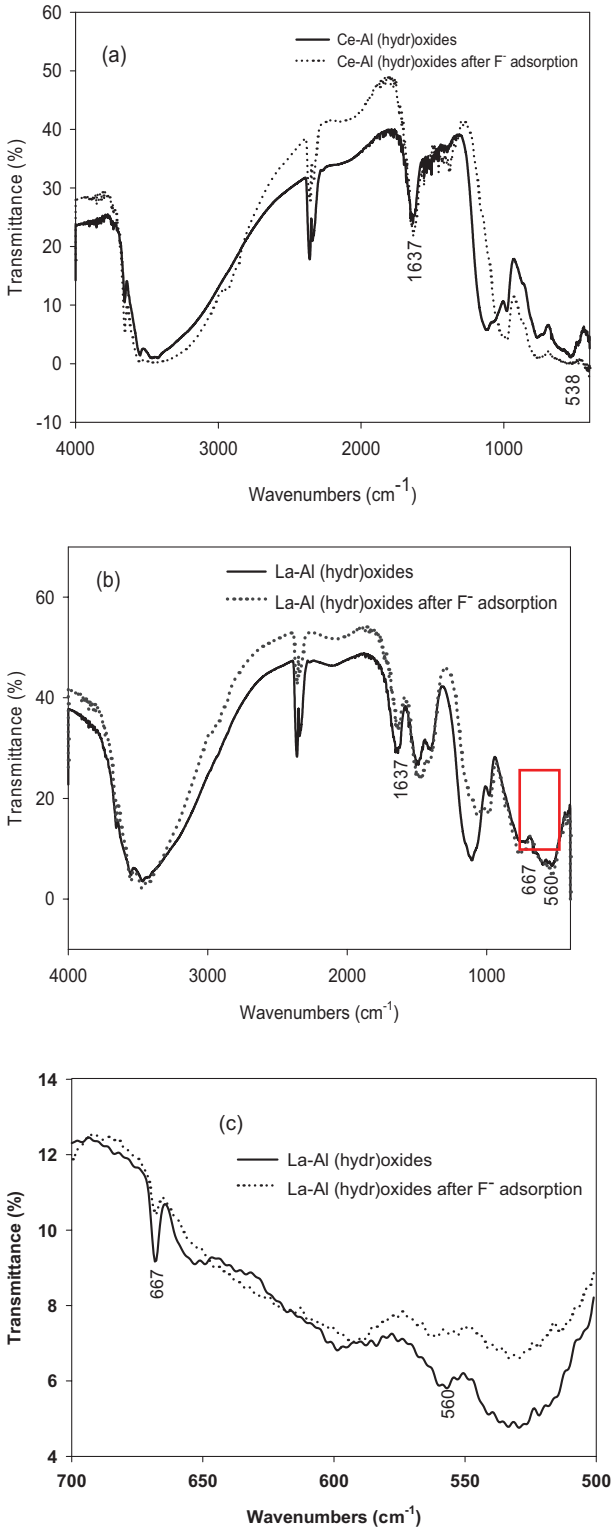

Fig. 10. FTIR spectra of (a) Ce–Al (hydr)oxides and (b) and (c) La–Al (hydr)oxides before and after fluoride adsorption.

above results confirmed that the Ce and La played a key role in fluoride adsorption on these two composites, while the main role for Al atoms was to form an amorphous structure.

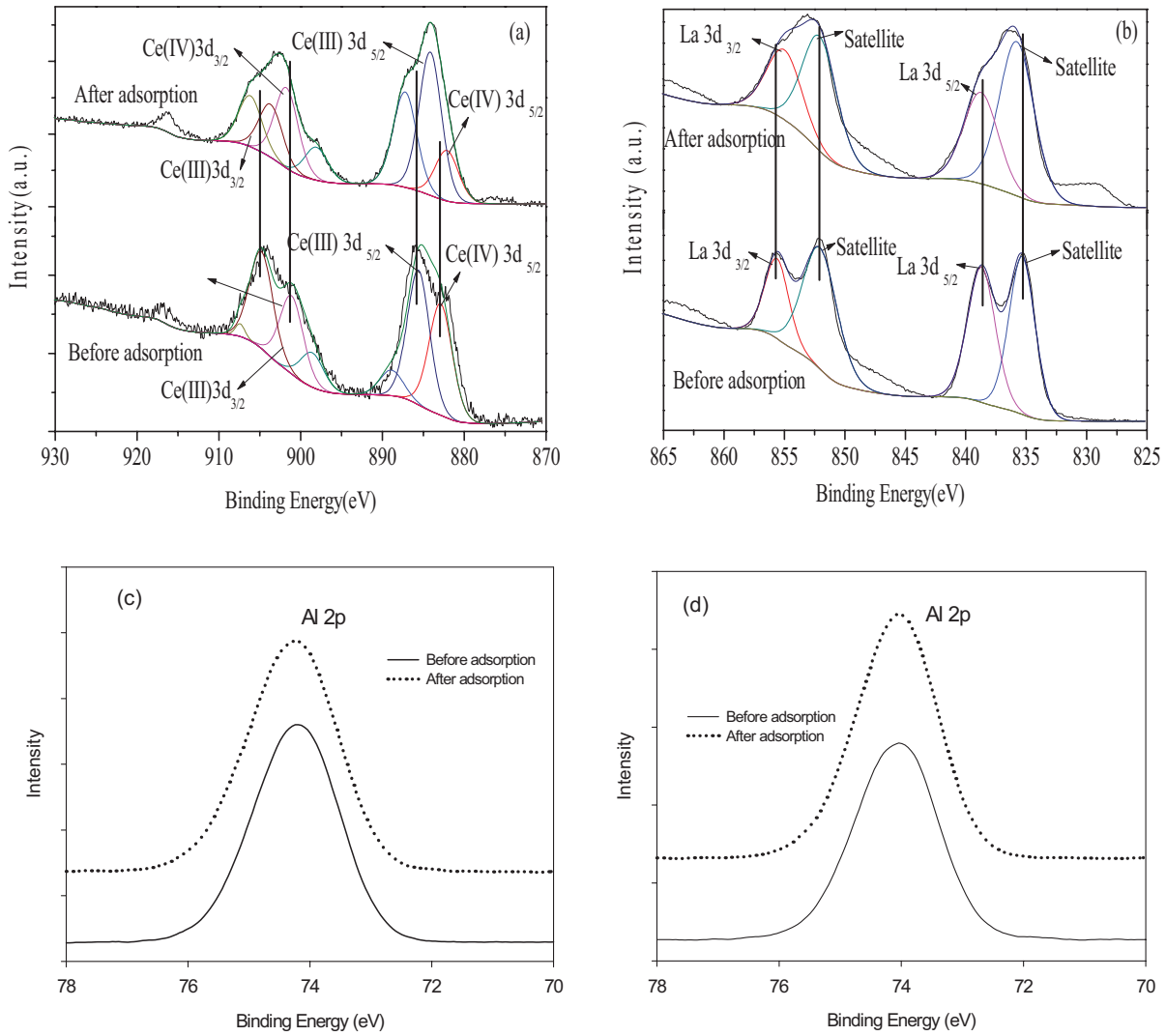

Fig. 11. XPS spectra of (a) Ce 3d for Ce–Al (hydr)oxides, (b) La 3d for La–Al (hydr)oxides, (c) Al 2p for Ce–Al (hydr)oxides and (d) Al 2p for La–Al (hydr)oxides before and after fluoride adsorption.

3.8. Treated water quality

A natural water sample collected from a lake in Central South University was spiked with 10 mg L^{-1} of fluoride and was treated with Ce–Al (hydr)oxides. The water quality parameters before and after treatment are presented in Table 5. Evidently, fluoride concentration was reduced significantly after Ce–Al (hydr)oxides treatment. Also, there is a significant reduction in the levels of other water quality parameters. It is evident from the results that Ce–Al (hydr) oxides can be effectively employed for removing the fluoride.

Table 5
Parameters of water before and after treated with Ce–Al (hydr) oxides (volume of water: 500 mL, Ce–Al (hydr)oxides dose: 1.0 g L^{-1}, contact time: 24 h)

Parameters	Untreated sample	Treated with Ce–Al (hydr) oxides
Turbidity (TU)	26	20
pH	8.03	8.05
Total organic carbon (mg L^{-1})	6.607	3.742
F^- concentration (mg L^{-1})	10.78	3.12
SO_4^{2-} concentration (mg L^{-1})	20.79	13.55
Cl^- concentration (mg L^{-1})	37.981	24.67

4. Conclusions

This study presented a facile-direct method to prepare various aluminum-based bimetallic (hydr)oxides including Mn, Zn, Cu, Ce and La. The electronegativity of the anchored metals played a key role in enhancing fluoride affinity toward the composites surface. Ce–Al (hydr)oxides and La–Al (hydr)oxides exhibited better performance for fluoride removal due to the lower electronegativity of Ce and La. Kinetic study results indicated that the fluoride adsorption over the Ce–Al (hydr)oxides and La–Al (hydr)oxides follows

a pseudo-second-order kinetic model. The Ce–Al (hydr) oxides showed an excellent fluoride adsorption capacity at a wide pH range of 4–11, indicating the applicability of this developed adsorbent for fluoride removal in natural water environment. The adsorption capacities of Ce–Al (hydr) oxides and La–Al (hydr)oxides for fluoride were 105.05 and 86.48 mg g^{-1} calculated from Langmuir model, respectively, higher than many reported adsorbents. Fluoride adsorption mechanism can be illustrated that both Ce and La atoms can act as a bridge between adsorbed fluoride and adsorbents surface, and played a key role in fluoride adsorption on these two composites. Results from this study demonstrate potential utility of the composites that could be developed into a viable technology for fluoride removal from water.

Acknowledgments

This work was financially supported by Changjiang Scholars Program of Ministry of Education of China-Distinguished Professor (T2011116) and National Natural Science Foundation of China (Grants 51304252 and 51774338).

References

[1] L. Wu, G. Zhang, D. Tang, A novel high efficient Mg–Ce–La adsorbent for fluoride removal: kinetics, thermodynamics and reusability, Desal. Wat. Treat., 57 (2016) 23844–23855.
[2] C. Zhang, Y. Li, T. Wang, Y. Jiang, H. Wang, Adsorption of drinking water fluoride on a micron-sized magnetic Fe_3O_4@Fe-Ti composite adsorbent, Appl. Surf. Sci., 363 (2016) 507–515.
[3] K. Jiang, K. Zhou, Y. Yang, H. Du, A pilot-scale study of cryolite precipitation from high fluoride-containing wastewater in a reaction-separation integrated reactor, J. Environ. Sci. (China), 25 (2013) 1331–1337.
[4] J.J. García-Sánchez, M. Solache-Ríos, V. Martínez-Miranda, C.S. Morelos, Removal of fluoride ions from drinking water and fluoride solutions by aluminum modified iron oxides in a column system, J. Colloid Interface Sci., 407 (2013) 410–415.
[5] H. Basu, R.K. Singhal, M.V. Pimple, A.V.R. Reddy, Synthesis and characterization of alumina impregnated alginate beads for fluoride removal from potable water, Water Air Soil Pollut., 224 (2013) 1572.
[6] A. Ghosh, K. Mukherjee, S.K. Ghosh, B. Saha, Sources and toxicity of fluoride in the environment, Res. Chem. Intermed., 39 (2013) 2881–2915.
[7] L.S. Thakur, P. Mondal, Techno-economic evaluation of simultaneous arsenic and fluoride removal from synthetic groundwater by electrocoagulation process: optimization through response surface methodology, Desal. Wat. Treat., 57 (2016) 28847–28863.
[8] Report on the State of the Environment in China, 2008.
[9] P.J. Sajil Kumar, P. Jegathambal, E.J. James, Factors influencing the high fluoride concentration in groundwater of Vellore District, South India, Environ. Earth Sci., 72 (2014) 2437–2446.
[10] K. Jiang, K.G. Zhou, Y.C. Yang, H. Du, Growth kinetics of calcium fluoride at high supersaturation in a fluidized bed reactor, Environ. Technol., 35 (2014) 82–88.
[11] D.-W. Cho, B.-H. Jeon, Y. Jeong, I.-H. Nam, U.-K. Choi, R. Kumar, H. Song, Synthesis of hydrous zirconium oxide-impregnated chitosan beads and their application for removal of fluoride and lead, Appl. Surf. Sci., 372 (2016) 13–19.
[12] W. Yang, Q. Tang, J. Wei, Y. Ran, L. Chai, H. Wang, Enhanced removal of Cd(II) and Pb(II) by composites of mesoporous carbon stabilized alumina, Appl. Surf. Sci., 369 (2016) 215–223.
[13] T. Wang, L. Zhang, C. Li, W. Yang, T. Song, C. Tang, Y. Meng, S. Dai, H. Wang, L. Chai, J. Luo, Synthesis of core–shell magnetic Fe_3O_4@poly(*m*-phenylenediamine) particles for chromium reduction and adsorption, Environ. Sci. Technol., 49 (2015) 5654–5662.
[14] M. Mouelhi, I. Marzouk, I. Marzouk, Optimization studies for water defluoridation by adsorption: application of a design of experiments, Desal. Wat. Treat., 57 (2016) 9889–9899.
[15] N.A. Oladoja, B. Helmreich, Batch defluoridation appraisal of aluminium oxide infused diatomaceous earth, Chem. Eng. J., 258 (2014) 51–61.
[16] J. Jiménez-Becerril, M. Solache-Ríos, I. García-Sosa, Fluoride removal from aqueous solutions by boehmite, Water Air Soil Pollut., 223 (2012) 1073–1078.
[17] C. Yang, L. Gao, Y. Wang, X. Tian, S. Komarneni, Fluoride removal by ordered and disordered mesoporous aluminas, Microporous Mesoporous Mater., 197 (2014) 156–163.
[18] A. Bansiwal, P. Pillewan, R.B. Biniwale, S.S. Rayalu, Copper oxide incorporated mesoporous alumina for defluoridation of drinking water, Microporous Mesoporous Mater., 129 (2010) 54–61.
[19] J.M. Chem, J. Zhou, Y. Cheng, G. Liu, Hierarchically porous calcined lithium/aluminum layered double hydroxides: facile synthesis and enhanced adsorption towards fluoride in water, J. Mater. Chem., 21 (2011) 19353–19361.
[20] D. Dayananda, V.R. Sarva, S.V. Prasad, J. Arunachalam, N.N. Ghosh, Preparation of CaO loaded mesoporous Al_2O_3: efficient adsorbent for fluoride removal from water, Chem. Eng. J., 248 (2014) 430–439.
[21] T. Zhang, Q. Li, Y. Liu, Y. Duan, W. Zhang, Equilibrium and kinetics studies of fluoride ions adsorption on CeO_2/Al_2O_3 composites pretreated with non-thermal plasma, Chem. Eng. J., 168 (2011) 665–671.
[22] S. Moriyama, K. Sasaki, T. Hirajima, Effect of calcination temperature on Mg–Al bimetallic oxides as sorbents for the removal of F^- in aqueous solutions, Chemosphere, 95 (2014) 597–603.
[23] S. Moriyama, K. Sasaki, T. Hirajima, Effect of freeze drying on characteristics of Mg–Al layered double hydroxides and bimetallic oxide synthesis and implications for fluoride sorption, Appl. Clay Sci., 132 (2016) 460–467.
[24] S.M. Maliyekkal, A.K. Sharma, L. Philip, Manganese-oxide-coated alumina: a promising sorbent for defluoridation of water, Water Res., 40 (2006) 3497–3506.
[25] J. Zhu, X. Lin, P. Wu, Q. Zhou, X. Luo, Fluoride removal from aqueous solution by Al(III)–Zr(IV) binary oxide adsorbent, Appl. Surf. Sci., 357 (2015) 91–100.
[26] X. Wu, Y. Zhang, X. Dou, B. Zhao, M. Yang, Fluoride adsorption on an Fe–Al–Ce trimetal hydrous oxide: characterization of adsorption sites and adsorbed fluorine complex species, Chem. Eng. J., 223 (2013) 364–370.
[27] W. Xiang, G. Zhang, Y. Zhang, D. Tang, J. Wang, Synthesis and characterization of cotton-like Ca–Al–La composite as an adsorbent for fluoride removal, Chem. Eng. J., 250 (2014) 423–430.
[28] J. Qiao, Z. Cui, Y. Sun, Q. Hu, X. Guan, Simultaneous removal of arsenate and fluoride from water by Al-Fe (hydr)oxides, Front. Environ. Sci. Eng., 8 (2014) 169–179.
[29] Y. Jia, B.-S. Zhu, K.-S. Zhang, Z. Jin, B. Sun, T. Luo, X.-Y. Yu, L.-T. Kong, J.-H. Liu, Porous 2-line ferrihydrite/bayerite composites (LFBC): fluoride removal performance and mechanism, Chem. Eng. J., 268 (2015) 325–336.
[30] L.M. Camacho, A. Torres, D. Saha, S. Deng, Adsorption equilibrium and kinetics of fluoride on sol-gel-derived activated alumina adsorbents, J. Colloid Interface Sci., 349 (2010) 307–313.
[31] C.R.N. Rao, J. Karthikeyan, Removal of fluoride from water by adsorption onto lanthanum oxide, Water Air Soil Pollut., 223 (2012) 1101–1114.
[32] T. Zhang, Q. Li, H. Xiao, Z. Mei, H. Lu, Y. Zhou, Enhanced fluoride removal from water by non-thermal plasma modified CeO_2/Mg–Fe layered double hydroxides, Appl. Clay Sci., 72 (2013) 117–123.
[33] J. Cheng, X. Meng, C. Jing, J. Hao, La^{3+}-modified activated alumina for fluoride removal from water, J. Hazard. Mater., 278 (2014) 343–349.
[34] W.L. Jolly, Modern Inorganic Chemistry, McGraw-Hill, New York, 1985.

[35] S. Deng, H. Liu, W. Zhou, J. Huang, G. Yu, Mn–Ce oxide as a high-capacity adsorbent for fluoride removal from water, J. Hazard. Mater., 186 (2011) 1360–1366.
[36] M.F. Rabiah Nizah, Y.H. Taufiq-Yap, U. Rashid, S.H. Teo, Z.A. Shajaratun Nur, A. Islam, Production of biodiesel from non-edible *Jatropha curcas* oil via transesterification using Bi_2O_3–La_2O_3 catalyst, Energy Convers. Manage., 88 (2014) 1257–1262.
[37] C. Gao, X.-Y. Yu, T. Luo, Y. Jia, B. Sun, J.-H. Liu, X.-J. Huang, Millimeter-sized Mg–Al-LDH nanoflake impregnated magnetic alginate beads (LDH-n-MABs): a novel bio-based sorbent for the removal of fluoride in water, J. Mater. Chem. A, 2 (2014) 2119.
[38] Y. Jia, B. Zhu, Z. Jin, B. Sun, T. Luo, X. Yu, L. Kong, J. Liu, Fluoride removal mechanism of bayerite/boehmite nanocomposites: roles of the surface hydroxyl groups and the nitrate anions, J. Colloid Interface Sci., 440 (2015) 60–67.
[39] W. Yang, S. Tian, Q. Tang, L. Chai, H. Wang, Fungus hyphae-supported alumina: an efficient and reclaimable adsorbent for fluoride removal from water, J. Colloid Interface Sci., 496 (2017) 496–504.
[40] S.S. Tripathy, J.L. Bersillon, K. Gopal, Removal of fluoride from drinking water by adsorption onto alum-impregnated activated alumina, Sep. Purif. Technol., 50 (2006) 310–317.
[41] K. Biswas, K. Gupta, A. Goswami, U.C. Ghosh, Fluoride removal efficiency from aqueous solution by synthetic iron(III)–aluminum(III)–chromium(III) ternary mixed oxide, Desalination, 255 (2010) 44–51.
[42] M. Bhaumik, T.Y. Leswifi, A. Maity, V.V. Srinivasu, M.S. Onyango, Removal of fluoride from aqueous solution by polypyrrole/Fe_3O_4 magnetic nanocomposite, J. Hazard. Mater., 186 (2011) 150–159.
[43] L. Chai, Y. Wang, N. Zhao, W. Yang, X. You, Sulfate-doped Fe_3O_4/Al_2O_3 nanoparticles as a novel adsorbent for fluoride removal from drinking water, Water Res., 47 (2013) 4040–4049.
[44] X. Zhao, D. Liu, H. Huang, W. Zhang, Q. Yang, C. Zhong, The stability and defluoridation performance of MOFs in fluoride solutions, Microporous Mesoporous Mater., 185 (2014) 72–78.
[45] E. Kumar, A. Bhatnagar, U. Kumar, M. Sillanpää, Defluoridation from aqueous solutions by nano-alumina: aharacterization and sorption studies, J. Hazard. Mater., 186 (2011) 1042–1049.
[46] Y. Fan, D. Fu, S. Zhou, Y. Lu, X. Zhao, W. Jin, Facile synthesis of goethite anchored regenerated graphene oxide nanocomposite and its application in the removal of fluoride from drinking water, Desal. Wat. Treat., 57 (2016) 28393–28404.
[47] Y. Zhang, X. Lin, Q. Zhou, X. Luo, Fluoride adsorption from aqueous solution by magnetic core-shell Fe_3O_4@alginate-La particles fabricated via electro-coextrusion, Appl. Surf. Sci., 389 (2016) 34–45.
[48] Y. Zhang, M. Yang, X.M. Dou, H. He, D.S. Wang, Arsenate adsorption on an Fe–Ce bimetal oxide adsorbent: role of surface properties, Environ. Sci. Technol., 39 (2005) 7246–7253.
[49] M. Aghazadeh, A.N. Golikand, M. Ghaemi, T. Yousefi, A novel lanthanum hydroxide nanostructure prepared by cathodic electrodeposition, Mater. Lett., 65 (2011) 1466–1468.